Reaction of OH + NO_2: High Pressure Experiments and Falloff Analysis†

Horst Hippler,* Nikolina Krasteva, Steffen Nasterlack, and Frank Striebel*

Lehrstuhl für Molekulare Physikalische Chemie, Universität Karlsruhe, Kaiserstrasse 12, D-76128 Karlsruhe, Germany

Received: October 31, 2005; In Final Form: March 9, 2006

High pressure experiments on the OH + NO_2 reaction are presented for 3 different temperatures. At 300 K, experiments in He ($p = 2-500$ bar) as well as in Ar ($p = 2-4$ bar) were performed. The rate constants obtained in Ar agree well with values which have been reported earlier by our group (Forster, R.; Frost, M.; Fulle, D.; Hamann, H. F.; Hippler, H.; Schlepegrell, A.; Troe, J. *J. Chem. Phys.* **1995**, *103*, 2949. Fulle, D.; Hamann, H. F.; Hippler, H.; Troe, J. *J. Chem. Phys.* **1998**, *108*, 5391). In contrast, the rate coefficients determined in He were found to be 15−25% lower than the values given in our earlier publications. Additionally, results for He as bath gas at elevated temperatures ($T = 400$ K, $p = 3-150$ bar; $T = 600$ K, $p = 3-150$ bar) are reported. The results obtained at elevated pressures are found to be in good agreement with existing literature data. The observed falloff behavior is analyzed in terms of the Troe formalism taking into account two reaction channels: one yielding HNO_3 and one yielding HOONO. It is found that the extracted parameters are in agreement with rate constants for vibrational relaxation and isotopic scrambling as well as with experimentally determined branching ratios. Based on our analysis we determine falloff parameters to calculate the rate constant for atmospheric conditions.

Introduction

Due to its importance in atmospheric chemistry the OH + NO_2 reaction has been the subject of many experimental and theoretical studies. In a recent data evaluation for atmospheric chemistry 22 studies are listed.[1] Despite the efforts made in the past there are still open questions (see also ref 1). In particular the following two questions have been discussed recently:

(i) What is the "best" set of falloff parameters (k_0, k_∞, F_c) to describe the pressure and temperature dependence of the rate constant?

(ii) What is the impact of HOONO formation on laboratory experiments, and what is the role of HOONO formation under atmospheric conditions?

Before we present our new experimental results, we will give a brief summary of the current knowledge on this reaction. Due to the large number of papers published we have to limit ourselves to those which are most relevant to this paper.

Until recently it has been assumed that OH and NO_2 react to form nitric acid as the only product:

$$OH + NO_2 + M \rightarrow HONO_2 + M \qquad (R1)$$

However, Robertshaw and Smith suggested already in 1982 that a second reaction channel leading to the formation of peroxynitrous acid,

$$OH + NO_2 + M \rightarrow HOONO + M \qquad (R2)$$

might interfere.[2] Early attempts to prove the HOONO formation in the reaction of OH + NO_2 failed.[3] These studies allowed only for estimating an upper bound for the HOONO yield which has been determined to be 10%. In 2000, Golden and Smith[4] as well as Matthieu and Green[5] published theoretical studies on the title reaction. The aim of these calculations was to model experimentally observed rate constants using statistical rate theory and taking into account both reaction channels. Golden and Smith concluded that HOONO formation might be considerable at low temperatures (~20%). This conclusion triggered new interest in this reaction, and different research groups attempted to detect HOONO as a reaction product. In 2001, Dransfield et al. tried to detect HOONO using FTIR spectroscopy. From their experimental observations they obtained no evidence for HOONO formation in the temperature range from 230 to 300 K and at pressures up to 375 Torr.[6] At the same time this group also published a paper on the isotopic scrambling of ^{18}OH in the reaction with NO_2,[7] and the authors claim that they have been able to obtain the high pressure limiting rate constant for HNO_3 formation. (We believe that this is not the case, and we will return to this point in the discussion.) The fact that the apparent high pressure rate coefficient extracted from these experiments is a factor of 5 lower than what has been reported by our group[8] led the authors of ref 7 to the conclusion that HOONO formation occurs at high pressures. The first experimental evidence for the formation of HOONO formation was reported in 2002 by Nizkodorov and Wennberg[9] and by our group.[10] The authors of ref 9 used an action spectroscopy technique to detect HOONO. We used a rather different approach using chemical kinetics instead of spectroscopy to prove the formation of different HNO_3 isomers.[10] By choosing proper conditions (elevated temperature and high pressures) we observed biexponential [OH] decays in the reaction of OH with NO_2. At the conditions of our experiments, HNO_3 is stable and, thus, the observation of a biexponential decay is only in agreement with the formation of a second, less stable reaction product. Based on the results of ab initio calculations (see, e.g., ref 11 and references cited therein) the only possibility is formation of HOONO. In 2003, Bean et al.[12]

† Part of the special issue "David M. Golden Festschrift".

* Corresponding authors. E-mail: horst.hippler@chemie.uni-karlsruhe.de; frank.striebel@chemie.uni-karlsruhe.de.

10.1021/jp0562734 CCC: $33.50
Published on Web 04/08/2006

detected HOONO as a reaction product in the OH + NO_2 reaction using IR-cavity ringdown spectroscopy. They determined the yield to be 7% at 300 K and a pressure of 20 Torr. Finally, D'Ottone et al. reported very recently the observations of biexponential [OH] decays in the OH + NO_2 reaction at 413 K and 400 Torr of He.[13] They also found that the observed biexponential decays are in agreement with a 10% yield of HOONO. In conclusion one might say that there is now ample experimental and theoretical evidence that HOONO is formed in the OH + NO_2 reaction. However, there is only little information available about the temperature and pressure dependence of the branching ratios between the competing reaction channels available.

So far, most experiments have been performed at temperatures below 400 K. At these temperatures, R1 and R2 compete. Since the branching ratio between these channels is not known, it is impossible to extract reliable falloff parameters for the two reactions from the experiments. One might use theory to calculate these parameters, and Troe[14] and Golden et al.[15] have recently published a theoretical analysis on the pressure and temperature dependence of the rate constants. It is, however, difficult to estimate the uncertainties of the statistical methods used in refs 14 and 15. Therefore, it seems to be desirable to have additional experimental data at hand in order to reduce the uncertainties of the falloff parameters for R1 and R2.

It is the aim of this study to present further experimental data to reduce existing uncertainties in the falloff parameters. Therefore we will present new high pressure data at room temperature for He. The motivation for these experiments is 2-fold: First, we reported indications that the rate coefficients published earlier by our group for He were roughly 30% too high.[10] Thus, we wanted to remeasure the rate coefficient for this reaction in order to reduce the uncertainties. We also checked our earlier results for Ar as bath gas as well as for He at 400 K, and these results are presented as well. A second motivation for the room temperature experiments comes from the fact that the rate for room temperature and $p \approx 1$ bar of N_2 (conditions typical for the lower troposphere) is remarkably uncertain. This is mainly due to the fact that D'Ottone et al.[16] reported a value for $p = 0.8$ bar which is roughly a factor of 1.7 higher than the one reported by Donahue et al.[17] The shape of falloff curves does hardly depend on the bath gas. Thus, even though our experimental results were obtained for He and Ar, it should be possible to reduce the existing uncertainties. Finally, we will present a falloff analysis of the rate constant. In order to check the extracted data against all information which is available, this is done in such a way, that not only thermal rate constants are taken into account but also rate constants reported for vibrational relaxation[13,18] and isotopic scrambling.[7,13,19] Since the falloff analysis is complicated by the pressure dependent branching between R1 and R2, rate coefficients for $T = 600$ K will be presented as well. At this temperature, HOONO formation can be excluded and the rate coefficients reported for $T = 600$ K should be used in the future to check falloff parameters for R1.

Experimental Procedures

The experimental setup has been described in earlier papers,[10,20] and we will therefore only describe the generation and the detection of OH radicals as well as typical experimental conditions.

The OH radicals were produced by pulsed laser flash photolysis of two different precursor molecules. Acetylacetone ($C_5H_8O_2$) was photolyzed at 248 nm, and nitric acid ($HONO_2$) was photolyzed at 248 or 193 nm. While nitric acid is a common precursor to generate OH radicals, acetylacetone has been—to the best of our knowledge—only used by our group in a kinetic study.[10] The photodissociation dynamics of acetylactone have been studied in ref 21.

The different photochemical systems provided a check that the method of OH radical preparation did not alter the kinetics. In all cases we used an excimer laser (Lambda Physik, Compex 201) for the photolysis with a typical laser fluence of 60 mJ/cm^2 at 248 nm and of 45 mJ/cm^2 at 193 nm. The OH radicals were detected using laser-induced fluorescence. We excited the radicals at 281.89 nm using a frequency doubled dye laser (Rhodamine 6 G, Lambda Physik, FL 3002), pumped by a frequency doubled Nd:YAG laser (Continuum PL7010) and by recording the nonresonant fluorescence at about 308 nm.

The reaction mixtures for the 248 nm photolysis contained as radical precursors typically 0.1 mbar of acetylacetone ($C_5H_8O_2$, Merck, >99%) or 1 mbar of nitric acid. The partial pressure of nitrogen dioxide (NO_2, Messer Griesheim, >98.0%) has been varied between 1 and 10 mbar, and the mixtures were completed with helium (Messer Griesheim, >99.999%) or Ar (Messer Griesheim, >99.999%). The mixtures for the 193 nm photolysis contained as radical precursor only 0.1 mbar of nitric acid. All gases were premixed in commercially available gas cylinders (Messer Griesheim, 40 dm^3, 300 bar) and were allowed to homogenize for at least 12 h. The pressure was measured using pressure gauges (Okhura Electric, 0−500 bar), and a flow of about 3 standard liters per minute was adjusted.

In some experiments, the NO_2 concentration in the gas mixture was measured directly in the gas flow with a UV absorption cell which was inserted into the high pressure gas flow directly behind the reaction cell. The UV absorption at 436 nm allowed for a continuous monitoring of the NO_2 concentration and therefore for a reduction of the experimental uncertainty.

Experimental Results and Kinetic Background

The analysis of the experimental results is based on the following assumptions: (i) OH is only consumed by reaction with NO_2, (ii) HNO_3 is thermally stable at the conditions of our experiments, and (iii) pseudo-first-order conditions are given. The recombination of OH is not taken into account due to the fact that $[NO_2] \geq 100 \times [OH]_0$. Moreover, the isomerization between HOONO and HNO_3 does not occur under the conditions of our experiment. Consequently, we are left with the following mechanism:

$$OH + NO_2 + M \rightarrow HONO_2 + M \qquad (R1)$$

$$OH + NO_2 + M \leftrightarrow HOONO + M \qquad (R2)$$

The kinetics of this mechanism is described by the following set of coupled differential equations:

$$\frac{d[OH]}{dt} = -(k_{1,1st} + k_{2,1st})[OH] + k_{-2}[HOONO] \qquad (1)$$

$$\frac{d[HOONO]}{dt} = k_{2,1st}[OH] - k_{-2}[HOONO] \qquad (2)$$

$k_{1,1st}$ and $k_{2,1st}$ are the pseudo-first-order rate constants for reaction R1 and R2, respectively, and k_{-2} is the rate constant

for the decomposition of HOONO. The solution of this equation system leads to the equation

$$[OH] = [OH]_0 \frac{(k_{-2} + s_1)}{s_1 - s_2} \exp(s_1 t) - [OH]_0 \frac{(k_{-2} + s_2)}{s_1 - s_2} \exp(s_2 t) \quad (3)$$

with the two eigenvalues

$$s_{1,2} = \frac{1}{2}\left(-(k_{-2} + (k_{1,1st} + k_{2,1st})) \pm \sqrt{(k_{-2} + (k_{1,1st} + k_{2,1st}))^2 - 4k_{1,1st}k_{-2}}\right) \quad (4)$$

s_1 is greater than s_2, and both eigenvalues are negative.

As discussed in our previous paper,[10] one has to expect biexponential decays. However, if the dissociation of HOONO occurs on a different time scale than the OH consumption, single exponential OH decays are observed. At low temperatures k_{-2} is much smaller than $k_{1,1st}$ and $k_{2,1st}$, thus one obtains

$$[OH] = [OH]_0 \exp(-(k_{1,1st} + k_{2,1st})t) \quad (5)$$

On the contrary, at high temperatures k_{-2} is much greater than $k_{1,1st}$ and $k_{2,1st}$. OH is then only consumed by reaction R1, and the following relation holds:

$$[OH] = [OH]_0 \exp(-k_{1,1st}t) \quad (6)$$

In this paper we present new data obtained at $T \leq 400$ K and results at $T = 600$ K and we use eq 5 and eq 6, respectively, to analyze and interpret our results. We shall mention at this point that the validity of either eq 5 or eq 6 is not connected with a distinct temperature range but it depends on both temperature and NO_2 concentration. So far, experiments on kinetics of the title reaction have been mostly performed at low temperatures and relatively high NO_2 concentrations. Under these conditions eq 5 is valid ($k_{1,1st}$, $k_{2,1st} \gg k_{-2}$). The results of those studies have then been used in atmospheric modeling studies. In the lower troposphere, however, the NO_2 concentrations are so low that eq 6 is valid (($k_{1,1st}$, $k_{2,1st} \ll k_{-2}$)) and OH + NO_2 react forming HNO_3 only. If one wants to measure the rate constant for this process, one should work under sufficiently high temperatures or low NO_2 concentrations so that either eq 3 or eq 6 describes the kinetics of the reaction.

The experimental results are summarized in Tables 1−4 (see Supporting Information). We did not observe any influence of the OH precursor on the extracted rate coefficient. Within the experimental uncertainties (which are estimated to be 30%), most of our new experimental results agree with what has been reported previously by us.[8] However, at 300 K the data obtained at pressures of a few bar (2−20 bar) are systematically lower (~25%) than the values given in ref 8. At higher pressures, the observed differences are smaller (15−20%). For $T = 400$ K and M = He as well as for $T = 300$ K and M = Ar, the experimental results reported in this work agree with the results from ref 8. For reasons of brevity, the data obtained in Ar as well as the data obtained in He at 400 K will not be discussed in detail in the remainder of the paper.

Discussion

To analyze the pressure and temperature dependence of the rate constants, thermodynamic data are necessary. For HNO_3 the information needed is well established, and for HOONO we could recently determine the equilibrium constant as a function of temperature in the range from 430 to 475 K.[10] In ref 10 we analyzed this data by performing a third-law analysis and extracted $\Delta H_r(0\ K)$ to be 83 kJ/mol. The analysis in ref 10 has been performed by calculating partition functions within the harmonic oscillator approximation and neglecting contributions of (hindered) internal rotations. However, the falloff analysis of this work indicated that contributions of internal rotations should be taken into account, and thus we reanalyzed the data of ref 10 to arrive at an internally consistent picture. The treatment of the internal rotation is based on the ab initio calculation by McGrath and Rowland.[22] (We note that there has been a more recent publication by the same authors[23] in which the barrier for the internal rotation is calculated to be higher. Adopting this higher value would have led to changes in the extracted heat of reaction smaller than 0.5 kJ/mol.)

We calculated the partition function for the internal rotation using the approximation proposed by Troe[24] and treating the potential energy surface (PES) for the rotation as a single well system. We tested this simplified procedure against a more sophisticated one proposed by Shokhirev and Krasnoperov.[25] The differences of the two procedures are found to be 5% or less in the temperature range of interest and thus less than the uncertainties arising from uncertainties of the PES for the internal rotation. For the sake of simplicity we therefore decided to stay with the method proposed by Troe.[24] Analyzing the temperature dependence of the equilibrium constant using this formalism yielded an O−O bond energy of $\Delta H°(0\ K) = (80.5 \pm 2)$ kJ/mol for the cis-cis isomer. This is in good agreement with recent theoretical predictions of (78.7 ± 4.2) kJ/mol[11] and (80.8 ± 1.7) kJ/mol[23] as well as with the value extracted by Golden et al.,[15] who analyzed our data and obtained a value of 82.1 kJ/mol. For the falloff analysis described below we stayed with the value obtained in this work in order to treat the internal rotor consistently with the same formalism in the third-law analysis as well as in the falloff analysis. The uncertainty in the threshold energy affects only the calculated strong collision rate constant noticeable. It leads to an uncertainty of the calculated density of states—and thus of the calculated low pressure rate constant—of roughly 10%. This uncertainty is smaller than the uncertainty introduced by the simplified treatments of anharmonic effects or internal rotors.

Falloff Analysis. We analyze the pressure dependence of the rate constants using the Troe formalism.[26] Within this model, the pressure dependent rate equation is given by the following equation:

$$\log\left(\frac{k}{k_\infty}\right) = \log\left(\frac{k_0/k_\infty}{1 + k_0/k_\infty}\right) + \frac{\log F_c}{1 + (\log(k_0/k_\infty)/N)^2} \quad (7)$$

$$N = 0.75 - 1.27 \log F_c$$

k_∞ and k_0 are the high and the low pressure limiting rate constants, respectively. F_c is the broadening factor. The strategy of the present analysis is as follows: we calculate the high pressure limiting rate constants for the two competing reactions using a simplified version of the statistical adiabatic channel model.[27] If our results are consistent with experimental observations (our own high pressure data, rate constants for vibrational relaxation, and isotopic scrambling), we proceed and calculate low pressure rate constants in the strong collision assumption. The analysis of the high and low pressure rate constants allows for a calculation of the strong and weak collision contributions, respectively, of the broadening factor F_c.

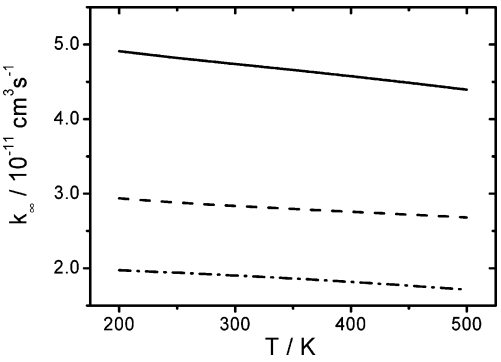

Figure 1. Calculated high pressure rate constants: $k_{1,\infty}$, dashed line; $k_{2,\infty}$, dashed dotted line; $k_{1,\infty} + k_{2,\infty}$, solid line.

High Pressure Rate Constant. We calculated the high pressure rate using a simplified version of SACM.[28,29] Within this model, the high pressure rate depends on the threshold energy, the frequencies of the reactants as well as the products, the frequency associated with the motion along the reaction coordinate, and a single interpolation parameter α. For HNO_3, the information needed is found, e.g., in ref 30. For HOONO, we used the frequencies calculated in ref 11 for *cis*,*cis*-HOONO and the threshold energy determined in this work. Thus we are left with a single parameter α. In ref 31 it was found that this parameter is typically half the Morse parameter β (which can be calculated easily) for the vibration which is associated with the motion along the reaction coordinate. Thus we did our calculations with $\alpha/\beta = 0.5$ and calculated the high pressure rates for R1 and R2 at 300 K to be 2.8×10^{-11} cm^3 s^{-1} and 1.9×10^{-11} cm^3 s^{-1}, respectively. A weak negative temperature dependence is predicted for both these rate constants (see Figure 1).

The sum of the two high pressure rate constants, which is the observable in high pressure experiments on the thermal reaction as well as in experiments of the vibrational relaxation of OH($v = 1$) in collisions with NO_2, is thus predicted to be 4.7×10^{-11} cm^3 s^{-1}. Experiments on the vibrational relaxation of OH(v=1) by NO_2 have been performed by Smith and Williams[18] as well as D'Ottone et al.,[16] and values of 4.8×10^{-11} cm^3 s^{-1} and 6.4×10^{-11} cm^3 s^{-1}, respectively, have been reported. The rate constants determined in this work at pressures above 200 bar are in the range from 5.0×10^{-11} cm^3 s^{-1} to 5.7×10^{-11} cm^3 s^{-1}. Due to the observed weak pressure dependence of the rate at these high pressures, it is estimated that these values deviate at most 20% from the high pressure limit. Our experimental high pressure results agree within the experimental uncertainties well with the results from studies on the vibrational relaxation as well as with our calculated high pressure rate constants. Taking into account all experimental information available on the sum of $k_{1,\infty}$ and $k_{2,\infty}$ we conclude that the calculated high pressure data are of sufficient accuracy and that no further optimization is needed.

At this point we shall also discuss the work by Donahue et al.,[7] in which the authors claim they were able to extract the high pressure limiting rate constant for HNO_3 formation from experiments on isotope exchange in the reaction $^{18}OH + NO_2$. This approach is based on the following idea: (i) if the rate for the isomerization of the chemically activated HNO_3 formed in the reaction R1,

$$H^{18}ONO_2^* \rightarrow HON^{18}OO^* \qquad \text{(R3)}$$

is much faster than the redissociation and (ii) if the chemically activated adduct is not stabilized by collisions, the rate constant for isotopic scrambling would be $(2/3)k_{1,\infty}$. The factor 2/3 stems from the fact that the H atom will be randomly localized at the 3 different O atoms. From their measured rate constant for isotopic scrambling Donahue et al. determined a high pressure rate of $k_{1,\infty} = 1.5 \times 10^{-11}$ cm^3 s^{-1}. Our experimental observations as well as the result of our SACM calculations indicate that the high pressure rate for R1 is higher. Therefore, we decided to check the validity of the assumptions mentioned above.

Donahue et al. did DFT calculations on a relatively low level to check the validity of the assumptions used. They found that the barrier for isomerization (R3) is about 18 kcal/mol lower than the one for the decomposition of HNO_3 (−R1). Using RRKM theory they calculated the rate for the isomerization reaction of chemically activated HNO_3 formed in reaction R1 and found it to be on the order of 10^{10} s^{-1}. The rate constant for back-dissociation was not calculated, but it was estimated from a simple Lindemann−Hinshelwood model:

$$k_0 = k_\infty \frac{\beta_c Z}{k_d} \qquad (8)$$

In this equation, k_0 and k_∞ are the low and the high pressure rate constant, respectively. Z is the second-order collision rate constant, and β_c is the collision efficiency. k_d is the rate constant for the dissociation of the chemically activated adduct, and it was calculated from eq 8 to be $\sim 8 \times 10^8$ s^{-1}. Based on this simple estimate the experiments of Donahue et al. should allow for a determination of $k_{1,\infty}$. We present here a more sophisticated approach to check if assumption (i) is valid. First we calculated initial distributions ($F(E)$) of the chemically activated HNO_3 formed in reaction R1 using the following relation:[32]

$$F(E) = \frac{W(E)\exp\left(\frac{-E}{k_B T}\right)}{\int_0^\infty W(E)\exp\left(\frac{-E}{k_B T}\right) dE} \qquad (9)$$

In this equation $W(E)$ is the number of open channels, which we obtained from our SACM calculations, E is the internal energy of the HNO_3 adduct, and k_B is the Boltzmann constant. Assuming that collisional stabilization can be neglected, we calculated mean rate constants for the reactions −R1 and R3 of the chemically activated HNO_3 from the following equation:

$$\langle k_i \rangle = \int_0^\infty k_i(E)\, F(E)\, dE \qquad (10)$$

The specific rate constants for reaction −R1 have been calculated using the SACM formalism as described above. The rate constants for reaction R3 have been calculated from RRKM calculations using the Whitten-Rabinovitch approximation for both density and sum of states of the reactant and transition state, respectively. We used a threshold energy of 33.5 kcal/mol, since Donahue et al. calculated this threshold to be 18 kcal/mol below the one for dissociation (−R1).[7] All other parameters used in the calculations of the rate constants for R3 have been adopted from ref 7.

A typical distribution as well as the specific rate constants for the two competing reaction channels is shown in Figure 2. For $J = 0$ we calculate mean rate constants of $\langle k_{-1} \rangle = 1.2 \times 10^{10}$ s^{-1} and $\langle k_3 \rangle = 9.3 \times 10^9$ s^{-1} at 300 K. Note that these rate constants are so fast that our initial assumption that collisional deactivation is unimportant holds for the conditions ($p \leq 220$

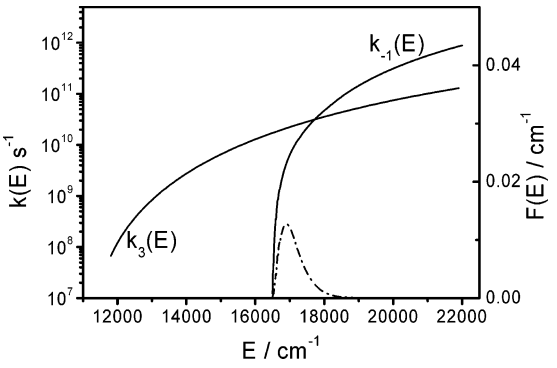

Figure 2. Calculated specific rate constants for the decomposition of HNO_3 ($k_{-1}(E)$) and the isomerization of HNO_3 ($k_3(E)$). The dashed dotted line is the initial distribution of the chemically activated HNO_3 formed in R1. See text for further explanations.

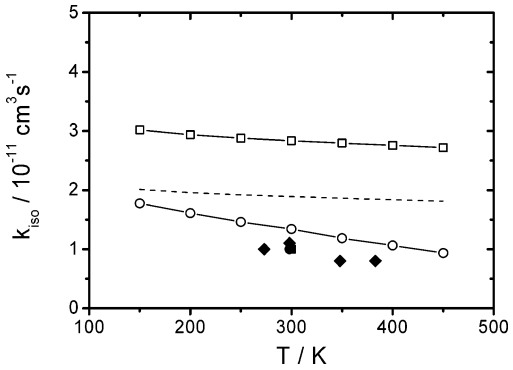

Figure 3. Calculated specific rate constants for the isotopic scrambling in the $^{18}OH + NO_2$ reaction (open circles) compared to literature data (●, ref 19; ■, ref 7; ◆, ref 16). For comparison, $k_{1,\infty}$ (open squares) and $(2/3)k_{1,\infty}$ (dashed line) are added as well. See text for further explanations.

Torr) of the experiments described in ref 7. We then set up a chemical model for the isotopic scrambling experiments which includes three HNO_3 isomers, of which two might decompose to form ^{16}OH and the third one decomposes to form ^{18}OH. Further on, we assumed that both $\langle k_{-1} \rangle$ and $\langle k_3 \rangle$ are the same for the different isomers. Within this model we calculated apparent rate constants for the isotopic scrambling from the [^{18}-OH] decay, and we compare these calculated rate coefficients in Figure 3 with the experimental results reported in the literature. Additionally, we added our calculated high pressure rate constant as well as $(2/3)k_{1,\infty}$. From Figure 3 it is seen that our model is able to predict the rate for isotopic scrambling with an accuracy of 35%. Additionally, a weak temperature dependence is predicted which is in agreement with the findings of ref 16. Thus, we conclude that our calculated high pressure rate constant for R1 is in agreement with the results from the isotopic scrambling experiments.[7,16,19] It has to be stressed that we used some simplifications in the model. E.g., the mean lifetimes have been calculated for $J = 0$. In order to check if the J dependence of the specific rate coefficients plays an important role, we performed the same calculations for $T =$ 300 K and $J = 20$, 35, and 50. It is found that the J dependence has only a minor effect (<10%) on the calculated rate constant for isotopic scrambling. The main uncertainty of our model arises from the fact that the threshold for R3 is not well-characterized. As long as this quantity has not been calculated with better ab initio methods, more sophisticated models seem not to be more meaningful.

Our calculations show that the assumption that the isomerization reaction is much faster than redissociation is not valid. The reason is that, due to the stronger energy dependence of the specific rate constants for −R1 compared to those for R3, the rate constants "cross" (vibrational channel switching, see also Figure 2). In other words, compared to R3, −R1 is getting faster with increasing excitation energy (increasing temperature). Only at temperatures well below 200 K the isomerization might be much faster than the back-dissociation. Thus, experiments on the isotopic scrambling at low temperatures should provide experimental access to the high pressure rate for R1. If the energetics for the isomerization reaction are better characterized, one might also be able to extract the high pressure limiting rate constant for HNO_3 formation from the temperature dependence of the rate coefficient for isotopic scrambling.

We conclude that our calculated high pressure rates are in agreement with the experimental data available (high pressure rate constants from this work, vibrational relaxation rate constants from refs 16 and 18, and rate constants for isotopic scrambling from refs 7, 16, and 19). Therefore, they should be sufficiently accurate and we can proceed with the calculations of the low pressure rate as well as the broadening factor.

Low Pressure Rate Constant and Broadening Factor. We analyze the low pressure rate constant using the formalism proposed by Troe.[24,26] To do this, we first calculate the strong collision rate constant for R1. Then we compare the calculated strong collision rate constant with experimental results and extract collision efficiencies. Next, we calculate strong collision rate constants for R2 and check if the observed pressure dependence for this reaction is consistent with our analysis. (Again the calculations are performed for *cis,cis*-HOONO.)

Within this model, the low pressure rate constant for a unimolecular reaction, which is related with the recombination rate constant via the equilibrium constant, is given by the following equation:

$$k_0^{sc} = Z_{LJ}[M]\frac{\rho_{vib,h}(E_0)k_B T}{Q_{vib}}\exp\left(-\frac{E}{k_B T}\right)F_{anh}F_E F_{rot}F_{rot\,int} \quad (11)$$

The calculation of the Lennard-Jones collision number (Z_{LJ}), the harmonic density of states ($\rho_{vib,h}$), the vibronic partition function (Q_{vib}), and the correction factor F_E is straightforward. There are, however, some uncertainties and problems associated with the calculation of the corrections factors F_{anh}, F_{rot}, and $F_{rot\,int}$. For the calculation of the factor F_{anh} we used the expression proposed in ref 24. Since then different ways to calculate F_{anh} have been proposed (see, e.g., refs 33 and 34). However, there is still no simple and yet "universal" formalism to calculate anharmonic density of states as well as correction factors to account for anharmonic effects. Thus we stay with the most simple and most commonly used way to calculate F_{anh}. The calculation of F_{rot} has been done as described in ref 28 (see also ref 14 for a discussion), and the calculations are based on centrifugal barriers calculated in the SACM calculations. The factor $F_{rot\,int}$ accounts for an increase of the density of states due to an internal rotor. While the calculations are relatively easy for one hindered internal rotor, there is no simple way to treat 2 different internal rotors. Thus, we calculated the contributions arising from the hindered "OH rotor" both in HNO_3 and in HOONO and neglected the "NO rotor" in the latter case.

One expects that in the low pressure regime reaction 1 is much faster than 2, and we thus first calculate the strong collision rate for this reaction and compare it to experimental

data. This comparison yields the collision efficiency β_c, which is given by the relation

$$\beta_c = \frac{k_0^{exp}}{k_0^{sc}} \tag{12}$$

and thus indirect information on the energy transfer process. The mean energy transferred per collision ($\langle\Delta E\rangle$) is related to the collision efficiency as follows:

$$-\langle\Delta E\rangle = \frac{\beta_c}{1-\sqrt{\beta_c}} F_E k_B T \tag{13}$$

From the analysis, we extracted $-\langle\Delta E\rangle$ for He, Ar, and N_2 at 300 K to be 20, 41, and 63 cm^{-1}, respectively. (The corresponding values for β_c at 300 K are 0.067, 0.12, and 0.17.) The temperature dependence of the extracted $-\langle\Delta E\rangle$ values was found to be weak (changes of $-\langle\Delta E\rangle$ smaller than 10% have been calculated in the T range from 220 to 400 K), and we thus assume temperature independent energy transfer parameters. Absolute values, trends of the changes in the energy transfer efficiency, and the independence of $-\langle\Delta E\rangle$ on the temperature are in agreement with the current knowledge on the still rather poorly characterized energy transfer processes.

For HOONO we assume that the energy transfer parameter $-\langle\Delta E\rangle$ for reaction R2 is the same as for reaction R1 and calculated the low pressure rate constants and the broadening factor as described above. Based on this assumption, a pressure dependence for k_2 is predicted which is not in agreement with our experimental results. If we instead choose $-\langle\Delta E\rangle = 80$ cm^{-1} for M = He, we obtain a good agreement between the calculated falloff curve and our experimental data. Note that Golden et al. observed as well better agreement between the results of a master equation calculation and experimental results when they assumed the energy transfer process for R2 to be more effective than the one for R1.[15] Compared to the $-\langle\Delta E\rangle$ value extracted for R1, this value seems to be too high. One has to admit, however, that this parameter is without doubt associated with a high uncertainty which arises from the treatment of the density of states. As long as there is no 2-dimensional potential energy surface for the two hindered internal rotors in HOONO available, one is not able to treat the density of states properly. On the other hand it should be kept in mind that (hindered) internal rotors—or low frequency modes—are believed to play a dominant role in collisional energy transfer. E.g., for a variety of colliders it has been found that $-\langle\Delta E\rangle$ for toluene is a factor of 2−4 larger than the corresponding value for benzene.[35] Since the two molecules are very similar, this finding has been explained by the presence of the internal rotor in toluene.

The extracted $\langle\Delta E\rangle$ values do have only little influence on the shape of the calculated falloff curves. Therefore, we content ourselves with the adjusted value and do not discuss it further. Additionally, we assume that $-\langle\Delta E\rangle$ for Ar and N_2 is 160 and 240 cm^{-1}, respectively. Having set this parameter and assuming that it is temperature independent, we are able to calculate the low pressure rate constant for R2 as a function of temperature.

The calculation of the broadening factor F_c is straightforward: For the strong collision contribution one has to analyze the temperature dependence of the transition state (pseudo-) partition function. The weak collision contribution is related to the collision efficiency. For N_2 as bath gas we calculate F_c to be 0.62 and 0.73 for R1 and R2, respectively. Again, the deduced temperature dependence is negligible. These values are higher than the ones discussed in the past;[8,14,15] however, they

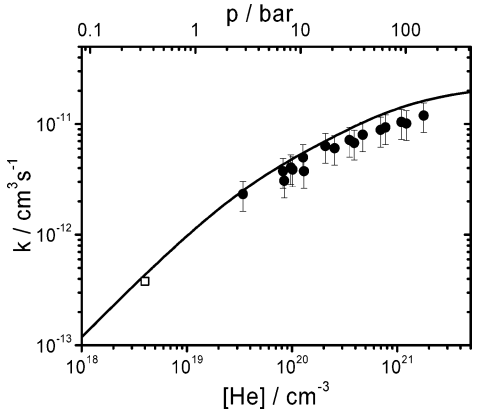

Figure 4. Falloff curve for helium at 600 K: ●, this work; □, ref 37; solid line, falloff curves calculated for R1 from eq 7; parameters for R1 are given in eq 14.

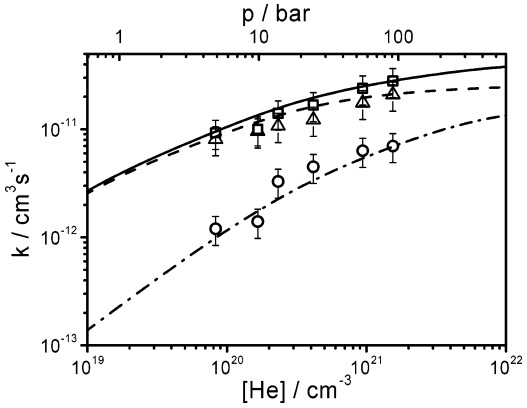

Figure 5. Falloff curve for helium at 430 K: △, k_1; ○, k_2; □, $k_1 + k_2$ (data are taken from ref 10); dashed and dashed dotted lines, falloff curves calculated from eq 7 for R1 and R2, respectively; solid line, sum of the two falloff curves. The falloff parameters for R1 and R2 are given in eq 14 and eq 15, respectively.

are reasonable and in agreement with current knowledge of this parameter. E.g., in ref 1 broadening factors ranging from 0.35 to 0.85 are reported for radical−radical reactions. It should be mentioned that for R2 F_c might well be smaller than predicted since there is some uncertainty associated with this value due to the fact that the extracted energy transfer efficiency might be too high.

Falloff Parameters. In this section we will limit the discussion on falloff parameters for He and N_2. The reason for this limitation is that most of the experimental data has been obtained using He as bath gas. N_2 is of course of practical interest and should thus be discussed as well.

For He, the following parameters are recommended:

$$k_{0,1} = 1.6 \times 10^{-30} \times (T/300\ \mathrm{K})^{-2.9}\ [\mathrm{He}]\ \mathrm{cm}^6\ \mathrm{s}^{-1} \quad \text{[ref 8]}$$
$$k_{\infty,1} = 2.8 \times 10^{-11}\ \mathrm{cm}^3\ \mathrm{s}^{-1} \tag{14}$$
$$F_{c,1} = 0.53$$

$$k_{0,2} = 4.6 \times 10^{-32} \times (T/300\ \mathrm{K})^{-2.8}\ [\mathrm{He}]\ \mathrm{cm}^6\ \mathrm{s}^{-1} \tag{15}$$
$$k_{\infty,2} = 1.9 \times 10^{-11}\ \mathrm{cm}^3\ \mathrm{s}^{-1}$$
$$F_{c,2} = 0.66$$

In Figures 4−6 we compare the falloff curves with experimental data for T = 600, 430, and 300 K, respectively. In all

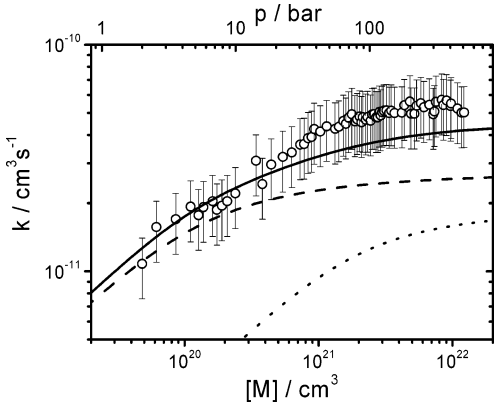

Figure 6. Falloff curve for helium at 300 K: ○, $k_1 + k_2$, this work; dashed and dotted lines, falloff curves calculated from eq 7 for R1 and R2, respectively; solid line, sum of the two falloff curves. The falloff parameters for R1 and R2 are given in eq 14 and eq 15, respectively.

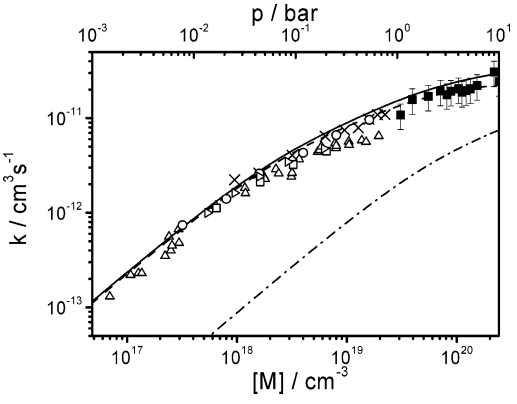

Figure 7. Falloff curve for nitrogen at 300 K: ○: Ref. 37; open triangle facing right, ref 38; △, ref 17; □, ref 39; ×, ref 16; dashed and dashed dotted lines, falloff curves calculated from eq 7 for R1 and R2, respectively; solid line, sum of the two falloff curves. The falloff parameters for R1 and R2 are given in eq 16 and eq 17, respectively. In order to compare the literature data for N_2 with our results obtained in He, we scaled the gas density for the latter data by a factor of 0.64 ($k_{0,He}/k_{0,N2}$) and added the results obtained in this way to the graph (■).

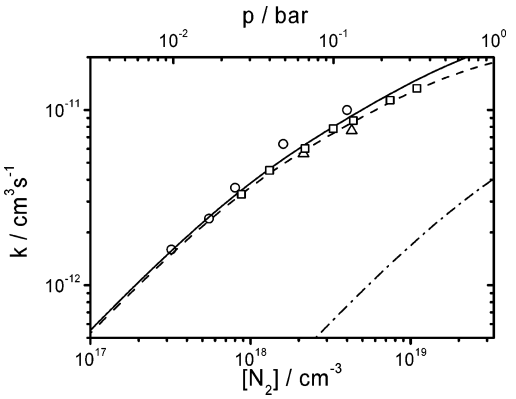

Figure 8. Falloff curve for nitrogen at 220 K: ○, ref 37; □, ref. 39; △, ref. 40; dashed and dashed dotted lines, falloff curves calculated from eq 7 for R1 and R2, respectively; solid line, sum of the two falloff curves. The falloff parameters for R1 and R2 are given in eq 16 and eq 17, respectively.

cases the experimental data agree reasonably well with the falloff parameters. At 600 K only HNO_3 formation occurs. For this temperature the calculated falloff overestimates the high pressure data (see Figure 4). Two reasons are possible: First, we might overestimate the broadening factor. Second, we might overestimate the high pressure limiting rate coefficient. This latter explanation would be in line with the finding that our simple model for the isotopic scrambling experiments overestimates the rate for this process. In Figure 5 we compare the data we extracted for k_1 and k_2 in a previous work at 430 K.[10] At this temperature, the calculated falloff curves agree with the experimental data within the uncertainties of the latter. Finally, we compare in Figure 6 our new data for $k_1 + k_2$ at high pressures and room temperature with the calculated falloff curves. Again we find that the agreement is within the experimental uncertainties. Similar agreement is found for $T =$ 400 K and for Ar as bath gas.[36] However, for lack of space we discuss neither these data in detail nor present the falloff curves. Instead, we will now turn to a discussion on the data available for nitrogen as collider. For this bath gas, the following falloff parameters have been obtained from our analysis:

$$k_{0,1} = 2.5 \times 10^{-30} \times (T/300\ \mathrm{K})^{-3.0}\ [\mathrm{N_2}]\ \mathrm{cm^6\ s^{-1}} \quad \text{[ref 16]}$$
$$k_{\infty,1} = 2.8 \times 10^{-11}\ \mathrm{cm^3\ s^{-1}} \qquad (16)$$
$$F_{c,1} = 0.62$$

$$k_{0,2} = 9.2 \times 10^{-32} \times (T/300\ \mathrm{K})^{-2.6}\ [\mathrm{N_2}]\ \mathrm{cm^6\ s^{-1}} \qquad (17)$$
$$k_{\infty,2} = 1.9 \times 10^{-11}\ \mathrm{cm^3\ s^{-1}}$$
$$F_{c,2} = 0.73$$

As we have already mentioned in the Introduction, discrepancies have been reported for nitrogen as bath gas and at room temperature. Thus, we should compare the result of our falloff analysis with experimental results in order to reduce the uncertainties. Basically, there are the results from Tony Hynes's group[16] and Ian Smith's group[37] which are at pressures above 100 Torr about 30% higher than data reported by Wine et al.,[38] Brown et al.,[39] and Donahue et al.[17] At pressures of 600 Torr, the difference between the data from ref 16 and ref 17 is even bigger (factor of 1.7). In Figure 7, we compare the experimental data available for N_2 and room temperature with the calculated falloff curves. For comparison, we added our high pressure results for M = He by scaling the gas densities by a factor of 0.64. The correction factor is calculated by dividing the low pressure rate constants for R1 and M = He by the one for M = N_2, and it accounts for the differences in the collision frequencies and collision efficiencies. This way of comparing data obtained in different bath gases has been applied before.[4,40] Both our new experimental results and our falloff analysis support the data from the Hynes group. A similar finding has been been found in the analysis performed by Golden et al.[15] This leads us to the conclusion that the data from ref 16 are more reliable than the data reported in ref 17. In order to further validate our falloff parameters we compare the calculated falloff curve for $T = 220$ K with experimental data (see Figure 8). The agreement obtained is rather satisfying. For $T = 240$ K and $T = 273$ K we as well obtained satisfying agreement.[36]

A final test for the falloff parameters comes from the comparison of predicted branching ratios with experimental data. In Figure 9, branching ratios for HOONO formation in N_2 at two different temperatures are shown. Our calculations predict that under atmospheric conditions less than 10% HOONO is formed. This prediction is in agreement with the first two studies on HOONO yields published.[3,6] More recently, Bean et al.[12] determined the HOONO yield to be ~7% at a pressure of 20 Torr and 300 K. (Note that these authors define the yield as

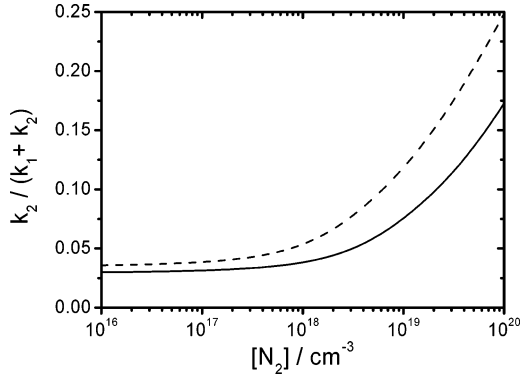

Figure 9. HOONO yield as a function of number density for two different temperatures: solid line, 300 K; dashed line, 220 K.

k_2/k_1 whereas our definition is $k_2/(k_1 + k_2)$.) Unfortunately, they did experiments in a mixture of N_2, Ar, and He (roughly 1:2:2), which makes the comparison with our analysis more difficult. At pressures of 20 Torr we predict from our analysis a yield of ~4%. This value is in quite fair agreement with the result from Bean et al. taking into account their uncertainty, which stems mainly from the fact that they have to rely on relative absorption cross sections from ab initio calculations. If we would try to match their yield, we would have to increase the low pressure rate constant for R2. Basically, we would have to increase the energy transfer parameter $-\langle\Delta E\rangle$. However, the extracted value for this parameter is a factor of 4 higher than the one we extracted for R1 and, thus, higher than expected.

To summarize this section on the falloff parameters: We have presented an analysis which—to the best of our knowledge—includes all experimental information available. In contrast to similar studies on the falloff behavior,[14,15] we have also discussed the isotopic scrambling experiments as well as our new high pressure data. The parameters extracted are—within experimental uncertainty—in agreement with the experimental data available. It is fair to note that for atmospheric modeling the falloff parameters from this work are probably not more accurate than the results from Troe[14] and Golden et al.[15] The rate coefficients $(k_1 + k_2)$ calculated with the different data sets for atmospheric conditions do agree within the uncertainty of the experimental data available. The main differences are in the branching ratios which are predicted to be ~2.5%,[14] ~10% (this work), or even ~15%[15] at 300 K and 1 bar of N_2. The experimental information about this quantity is still very limited, and more experiments seem to be needed. Additionally, high temperature (500−800 K) data on the rate constant would allow for a more precise determination of the falloff parameters for R1 and, thus, more experiments under these conditions seem to be desirable as well.

Conclusion

We have presented new high pressure data for the rate constant of the title reaction which should be used in further falloff analyses. Additionally, an analysis of the pressure dependence of the rate constant is given. The analysis allowed for an extraction of falloff parameters which are in agreement with most of the experimental data available so far. This data includes results not only from studies on the thermal rate constant but also from studies on the vibrational relaxation as well as isotopic scrambling and experiments aimed on a determination of the product branching ratios in the title reaction.

Acknowledgment. At the early stages of this work we enjoyed the stimulating and interesting discussion we had with Dave Golden during his stay in Karlsruhe in 2000. We thank Dave for his continued interest in our work and many discussions we had over the past few years.

Supporting Information Available: Four tables of experimental results. This material is available free of charge via the Internet at http://pubs.acs.org.

References and Notes

(1) Atkinson, R.; Baulch, D. L.; Cox, R. A.; Crowley, J. N.; Hampson, R. F.; Hynes, R. G.; Jenkin, M. E.; Rossi, M. J.; Troe, J. *Atmos. Chem. Phys.* **2004**, *4*, 1461.

(2) Robertshaw, J. S.; Smith, I. W. M. *J. Phys. Chem.* **1982**, *86*, 785.

(3) Burkholder, J. R.; Hammer, P. D.; Howard, C. J. *J. Phys. Chem.* **1987**, *91*, 2136.

(4) Golden, D. M.; Smith, G. P. *J. Phys. Chem. A* **2000**, *104*, 3991.

(5) Matheu, D. M.; Green, W. H. *Int. J. Chem. Kinet.* **2000**, *32*, 245.

(6) Dransfield, T. J.; Donahue, N. M.; Anderson, J. G. *J. Phys. Chem. A* **2001**, *105*, 1507.

(7) Donahue, N. M.; Mohrschladt, R.; Dransfield, T. J.; Anderson, J. G.; Dubey, M. K. *J. Phys. Chem. A* **2001**, *105*, 1515.

(8) Forster, R.; Frost, M.; Fulle, D.; Hamann, H. F.; Hippler, H.; Schlepegrell, A.; Troe, J. *J. Chem. Phys.* **1995**, *103*, 2949. Fulle, D.; Hamann, H. F.; Hippler, H.; Troe, J. *J. Chem. Phys.* **1998**, *108*, 5391.

(9) Nizkodorov, S. A.; Wennberg, P. O. *J. Phys. Chem. A* **2002**, *106*, 855.

(10) Hippler, H.; Nasterlack, S.; Striebel, F. *Phys. Chem. Chem. Phys.* **2002**, *4*, 2959.

(11) Li, Y.; Francisco, J. S. *J. Chem. Phys.* **2000**, *113*, 7976.

(12) Bean, B. D.; Mollner, A. K.; Nizkorodov, S. A.; Nair, G.; Okumura, M.; Sander, S. P.; Peterson, K. A.; Francisco, J. S. *J. Phys. Chem. A* **2003**, *107*, 6974.

(13) D'Ottone, L. D.; Bauer, D.; Campuzano-Jost, P.; Fardy, M.; Hynes, A. J. *Faraday Discuss.* **2005**, *130*, 111.

(14) Troe, J. *Int. J. Chem. Kinet.* **2001**, *33*, 878.

(15) Golden, D. M.; Barker, J. R.; Lohr, L. L. *J. Phys. Chem. A* **2003**, *107*, 11057 (see also the erratum: *J. Phys. Chem. A* **2004**, *108*, 8852).

(16) D'Ottone, L.; Campuzano-Jost, P.; Bauer, D.; Hynes A. J. *J. Phys. Chem. A* **2001**, *105*, 10538.

(17) Donahue, N. M.; Dubey, M. K.; Mohrschladt, R. D.; Demerijan, K. L.; Anderson, J. G. *J. Geophys. Res.* **1997,** *102*, 5.

(18) Smith, I. W. M.; Williams, M. D. *J. Chem. Soc., Faraday Trans. 2* **1985**, *81*, 1849.

(19) Grennblatt, G. D.; Howard, C. J. *J. Phys. Chem.* **1989**, *93*, 1035.

(20) Ausfelder, F.; Hippler, H.; Striebel, F. *Z. Phys. Chem.* **2000**, *214*, 403.

(21) Upadhyaya, H. P.; Kumar, A.; Naik, P. D. *Chem. Phys.* **2003**, *118*, 2590.

(22) McGrath, M. P.; Rowland, F. S. *J. Phys. Chem.* **1994**, *98*, 1061.

(23) McGrath, M. P.; Rowland, F. S. *J. Chem. Phys.* **2005**, *122*, 134312.

(24) Troe, J. *J. Chem. Phys.* **1977**, *66*, 4745. Troe, J. *J. Chem. Phys.* **1977**, *66*, 4758.

(25) Shokhirev, N. V.; Krasnoperov, L. N. Program Quantum Rotator, download page: http://www.chem.arizona.edu/faculty/walk/nikolai/programs.html (accessed Feb 2003).

(26) Troe, J. *J. Phys. Chem.* **1978**, *83*, 114.

(27) Quack, M.; Troe, J. *Ber. Bunsen-Ges. Phys. Chem.* **1974**, *78*, 240.

(28) Troe, J. *J. Chem. Phys.* **1981,** *75*, 226.

(29) Troe, J. *J. Chem. Phys.* **1983,** *79*, 6071.

(30) Mélen, F.; Herman, M. *J. Phys. Chem. Ref. Data* **1992**, *21*, 831.

(31) Cobos, C. J.; Troe, J. *J. Chem. Phys.* **1985**, *83*, 1010.

(32) Forst, W. *Theory of Unimolecular Reactions*; Academic Press: New York, 1973.

(33) Troe, J. *Chem. Phys.* **1995**, *190*, 381.

(34) Song, K.; Hase, W. L. *J. Chem. Phys.* **1999**, *110*, 6198.

(35) Toselli, B. M.; Barker, J. R. *J. Chem. Phys.* **1992**, *97*, 1809.

(36) Nasterlack, S.; Bestimmung von Ausbeuten bei komplexbildenden bimolekularen Reaktionen mittels laserinduzierter Fluoreszenz. Ph.D. Thesis, Karlsruhe, 2003.

(37) Anastasi, C.; Smith, I. W. M. *J. Chem. Soc., Faraday Trans. 2* **1976**, *72*, 1459.

(38) Wine, P. H.; Kreutter, N. M.; Ravishankara, A. R. *J. Phys. Chem.* **1979**, *83*, 3191.

(39) Brown, S. S.; Talukdar, R. K.; Ravishankara, A. R. *Chem. Phys. Lett.* **1999**, *299*, 277.

(40) Dransfield, T. J.; Perkins, K. K.; Donahue, N. M.; Anderson, J. G.; Sprengnether, M. M.; Demerijan, K. L. *Geophys. Res. Lett.* **1999,** *26*, 687.